NOTES AND CORRESPONDENCE

Signature of Lighthouses, Ships, and Small Islands in Altimeter Waveforms

J. TOURNADRE

Département d'Océanographie Physique et Spatiale, IFREMER, Plouzané, France

(Manuscript received 17 August 2005, in final form 11 September 2006)

ABSTRACT

High-rate (20 Hz) altimeter echo waveforms are particularly sensitive to small-scale changes of surface backscatter and they contain a wealth of information on the sea surface. A detailed analysis of these waveforms often reveals the signatures of objects that emerge from the sea. Such objects, such as beacons, lighthouses, ships, and small islands, have deterministic signatures that can be estimated using simple geometry. Examples of signatures of ships, beacons, and islands in the TOPEX/Poseidon and Jason altimeters waveforms are presented and analyzed. Some potential applications are also presented.

1. Introduction

Spaceborne radar altimeters have been in use for almost 30 yr. The concepts underlying their operation are well known and have been extensively studied. The radar emits a short electromagnetic pulse, which is reflected by the sea surface. The waveform, that is, the shape and strength of the return echo, is recorded on the satellite. Geophysical parameters of the ocean surface, mainly, the sea surface height, the significant wave height, and the sea surface backscatter, are then derived from the analysis of the echo waveforms (Brown 1977). The use of these geophysical parameters is now widely spread among the scientific community and radar altimetry can be considered as a standard tool for oceanography. However, very few studies have been devoted outside the instrument design community to the analysis of high-rate altimeter echo waveforms over the ocean. High-rate altimeter waveforms have been used in various nonocean applications, such as sea ice mapping, ice caps, and inland lakes studies (Legresy et al. 2005). These data contain a wealth of information on the sea surface and are particularly sensitive to small-scale changes of surface backscatter caused, for example, by rain cells or surface slicks (Tournadre 1998; Quartly 1998; Tournadre et al. 2006). Their analysis reveals the presence of V-shaped patterns, characteristics of small-scale changes of surface backscatter. Such patterns are sometimes only discernible in the thermal noise section of the waveforms, that is, above mean sea level and wave crests. In such cases, small reflective targets that emerge from the sea, such as beacons, lighthouses, ships, and small islands or islets, most probably cause these patterns. These targets have deterministic signatures that can be easily computed by geometric consideration. These computations are similar to the ones used to estimate the altimeter waveforms over the transponders used for the calibration and validation of height and backscatter coefficient (Denys et al. 1995; Roca et al. 2003).

The study of these signatures might appear anecdotal, but several applications can be foreseen, such as the determination of the satellite ground track positioning, the estimation of ship traffic, or the improvement of the land mask used to flag the data. Section 2 presents the signature of a point target as well as its echo waveform. The next three sections (3 to 5) present the analysis of the signature of ships, beacons, and islands. The final section presents the potential applications.

2. Signature of point targets in altimeter waveforms

The backscatter coefficient of the echo waveform can be expressed as a double convolution product of the radar point target response, the flat sea surface re-

Corresponding author address: J. Tournadre, IFREMER, Technopole Brest-Iroise, 29280 Plouzané, France.
E-mail: jean.tournadre@ifremer.fr

DOI: 10.1175/JTECH2030.1

sponse, and the joint probability density function of slope and elevation of the sea surface (Brown 1977). The radar cross section for backscatter as a function of time $\sigma(t)$ for an altimeter pulse and for a Gaussian random distribution of rough-surface specular points can be expressed as (Barrick and Lipa 1985)

$$\sigma(t) = \frac{1}{2}(2\pi)^{3/2}H''\sigma_\tau\sigma_0\left[1 + \mathrm{erf}\left(\frac{x}{\sqrt{2}\sigma_p}\right)\right]e^{-\frac{x}{u_b}}, \tag{1}$$

where $x = ct/2$, $H'' = H/(1 + H/a)$ is the reduced satellite height, a is the earth's radius, and H is the satellite height. Here σ_τ is the standard deviation of the altimeter pulse; $\sigma_p = \sqrt{h^2 + \sigma_\tau^2}$, where h is the rms wave height; u_b is the antenna pattern standard deviation; and σ_0 is the target backscatter coefficient. It should be noted that the $t = 0$ corresponds to the mean sea level. The measured waveforms are given in telemetry samples of 3.125-ns width (the length of the pulse) and the nominal track point (i.e., the sea level or $t = 0$) is in general shifted to bin 32.5 (for TOPEX and Jason altimeters).

In a computation similar to the one presented by Denys et al. (1995) and Roca et al. (2003) for transponder, it can be easily shown by simple geometry that a point target (such as a lighthouse or a ship) of height δ above sea level located at distance d from the satellite nadir will give an echo at the time t_0 defined by

$$\frac{ct_0}{2} = -\delta + \frac{1}{2}\frac{a + H}{aH}d^2 = -\delta + \frac{d^2}{2H''}. \tag{2}$$

The echo waveform of a point target is purely deterministic. Using the radar equation over a transponder (Roca et al. 2003) and assuming Gaussian antenna pattern and altimeter pulse, it is of the form

$$\sigma_{\text{target}}(t) = \frac{\sigma_1}{2\pi^2 H^4\left(1 + \dfrac{d^2}{2H^2}\right)}e^{-\frac{u_0}{u_b}}e^{-\frac{(x-\delta+u_0)^2}{2\sigma_\tau^2}}, \tag{3}$$

where σ_1 is the target radar cross section and $u_0 = d^2/2H''$.

The characteristics of the different altimeters used in this study are given in Table 1.

A first condition for a target to be detectable in altimeter echo waveforms is that time t_0 lies within the time range during which the echo waveform is integrated. For example, a 10-m-high target can be seen for distances from nadir between 0 and 10 km. A 200-m-high small hilly island can be seen in echo waveforms as far as 25 km from nadir. A second necessary condition for detection is that the target backscatter coefficient must be large enough to come out of the background sea surface backscatter. Small targets, such as lighthouses or ships, whose radar cross sections are small will thus be detectable only in the thermal noise section of the echo waveform before the leading edge, that is, above the mean sea level. A wider target, such as a small island, which has a much stronger backscatter, might certainly be detected in any part of the waveform and cause tracker and data losses.

TABLE 1. Operating characteristics of altimeters.

Altimeter	TOPEX Ku	Poseidon Ku	Jason Ku
Launch date	10 Aug 1992	10 Aug 1992	7 Dec 2001
Altitude (km)	1334	1334	1334
Inclination	66°	66°	66°
Beamwidth	1.1°	1.1°	1.25°
Frequency (GHz)	13.60	13.65	13.575
PRF (Hz)	4200	1700	1800
Bin width (ns)	3.125	3.125	3.125
Waveform frequency (Hz)	10	20	20
No. of waveforms in average	456	86	90

3. Ships

The analysis of high-rate waveforms from Jason and TOPEX for several passes reveals that ships' echoes are frequently detected in both Ku- and C-band data. The signatures are in general weaker at C band because of a relative weaker reflection from point target. Ships' echoes are sometimes strong enough to cause tracker losses and erroneous data. Two examples of ships' signatures in Jason and TOPEX/Poseidon data are presented in Figs. 1 and 2. To ensure that the observed patterns are indeed caused by ships, the waveforms for the same pass and location but for different cycles were searched for the same patterns. The absence of signatures in these cycles shows that ships most probably caused the observed signatures. The first example shows a ship detected in the Mediterranean off the coast of Catalonia. The ship signature presents, as expected from (2), a parabolic shape. It is obvious from (2) that it is impossible to separate the information on ship height and off nadir distance from the signature alone. However, assuming that the ship is located at satellite nadir near 41.90°N, the best fit of the parabola gives a ship height of 12 m. This is the minimum height of the ship. The echo is strong enough near 41.91° to cause a tracker loss during six consecutive waveforms.

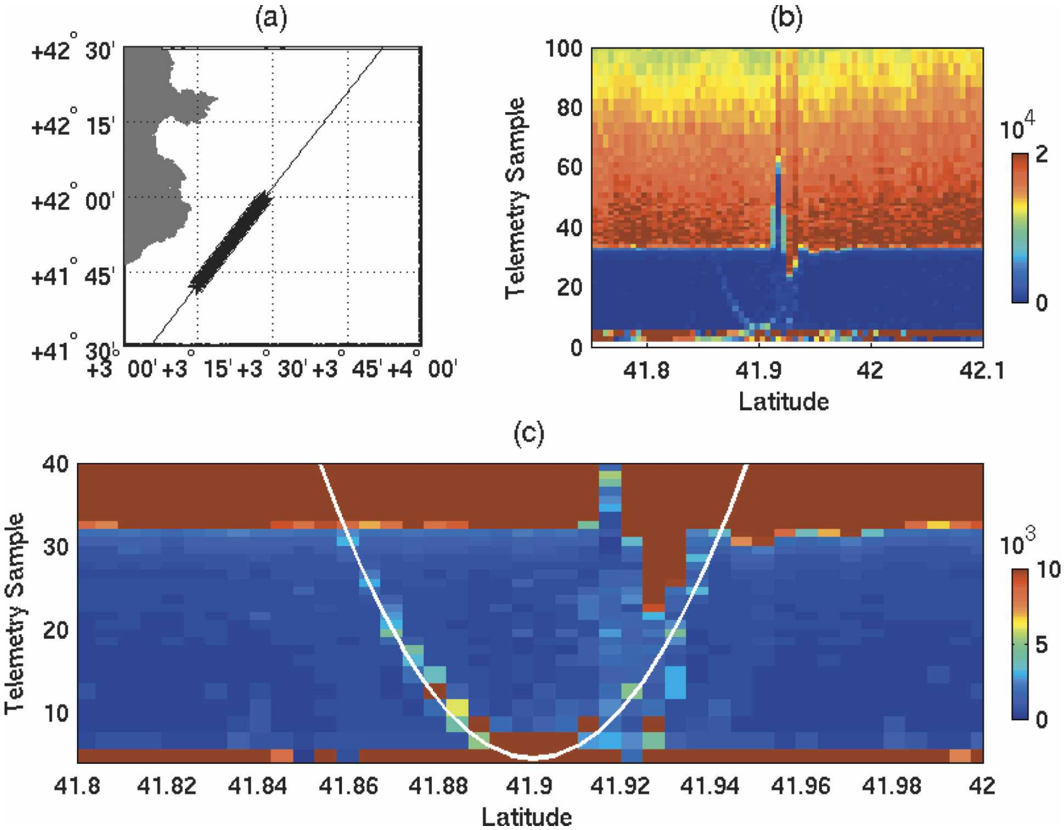

FIG. 1. Ship detection off the coast of Catalonia (Spain) in TOPEX cycle 332 pass 187. (a) Satellite ground track; (b) TOPEX altimeter 20-Hz waveforms; (c) detail of the waveforms showing the ship signature. The waveforms are given in arbitrary units.

The second case presents an example of double signature. As can be seen in the figure, two parabolas are clearly visible in the waveforms in the thermal section of the waveforms. This kind of pattern is often observed in the ship echoes. The presence of two echoes collocated in latitude indicates the presence of reflecting surfaces at two different altitudes. The most likely explanation is that in some cases the bridge and the deck

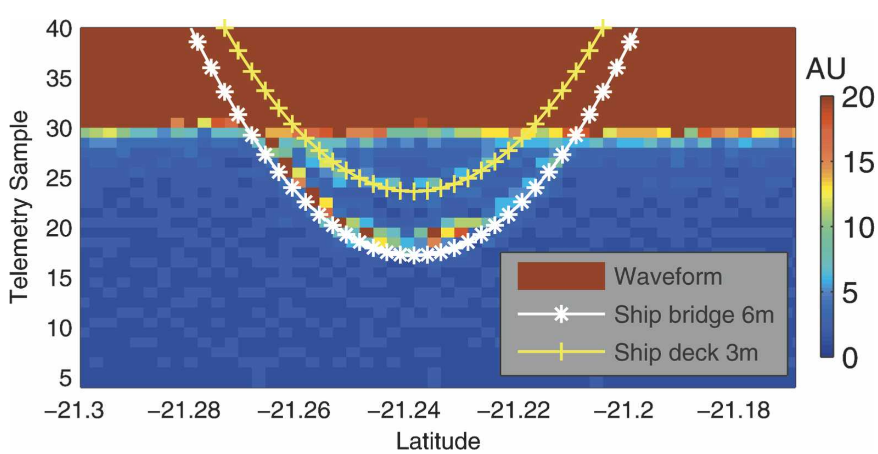

FIG. 2. Example of a double signature showing a ship bridge and deck detected in Jason high-rate waveforms off the coast of Australia near 21.2°S and 154°E; Jason cycle 9 pass 112.

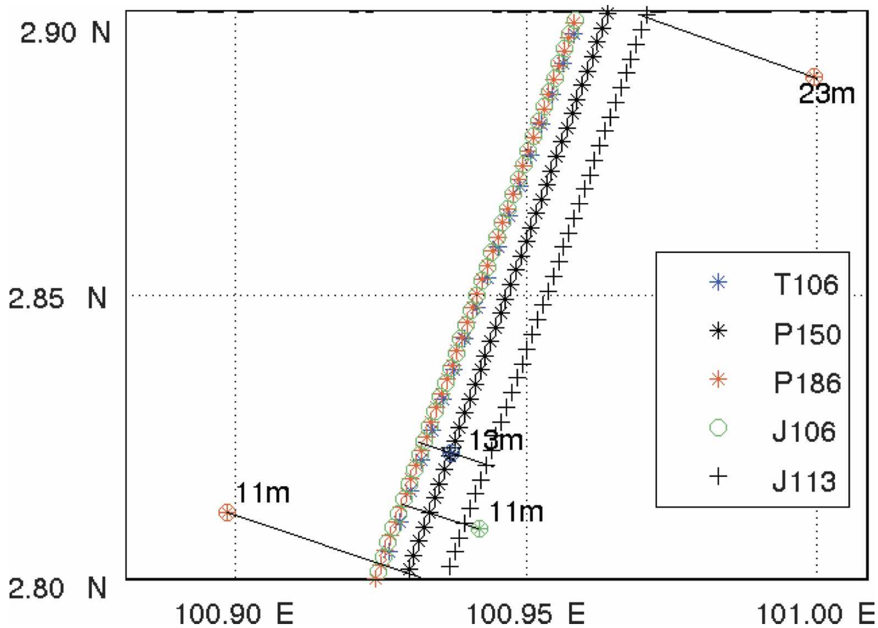

FIG. 3. Locations of beacons (circles and stars) in the Straits of Malacca and satellite ground tracks: TOPEX cycle 106 (blue stars); Poseidon cycle 150 (black stars); Poseidon cycle 186 (red stars); Jason cycle 106 (green circles); and Jason cycle 113 (black pluses).

of a ship can lead to two separate signatures. In this particular case, assuming that the ship lies at the satellite nadir, the best fit of the two echoes gives a 6-m high bridge and a 3-m high deck.

4. Beacons in the Straits of Malacca

The most striking example of point target signatures found in the TOPEX and Jason archive is located in the Straits of Malacca. There, several beacons signal shoal and sea lanes and luckily, the first orbit per cycle of TOPEX and Jason passes over a triangle formed by three beacons about 11 m high (see Fig. 3). These beacons are equipped with radar reflectors and have thus a quite high radar cross section so that, in spite of their small size, their signature is often detectable in the high-rate altimeter waveforms. It should be noted that as the waveforms are normalized by the altimeter automatic gain control, if the sea surface backscatter is high (such as in case of very calm sea) the beacons' signatures can become undetectable in the waveforms.

Figure 4 presents one TOPEX (Ku band), two Poseidon, and two Jason Ku-band high-rate waveforms over the beacons. The signatures of the beacons computed using (2) from the beacons and satellite data coordinates are superimposed on the waveforms. The permanence of the presence of echoes at an almost constant latitude and the good agreement between the waveforms and the expected beacons' signatures shows that the echoes are certainly caused by the beacons and not by ships.

The two northernmost beacons are never detected because their strongest signatures, that is, when they are at the nearest from the satellite nadir, lay in the first telemetry samples where there exists a "wraparound" problem resulting in an artificial rise of the return power at the beginning of the waveforms (Quartly et al. 2001). The two other beacons have better defined signatures, although they are not always both completely discernible. The eastern one is detected by Poseidon and not by Jason, while the western one is detected by TOPEX and Jason and not by Poseidon. The Poseidon cycle 186 waveforms are more complex. Three V-shaped patterns can be seen, two strong ones near 2.8275°N and a weak one near 2.8°N. Most probably, the weak one is associated with the western beacon and one of the strong ones with the eastern beacon, while the third is a ship's signature. The presence of ships is not surprising considering the ships' traffic in the Straits of Malacca. Others' ship signatures can also be seen in the waveforms for Poseidon cycle 150 near 2.875°N and for Jason cycle 106 near 2.775°N.

The comparison of the expected signatures to the observed waveforms reveals slight shifts in both latitude and telemetry sample [which correspond to a distance from nadir track using (2)]. These shifts in lati-

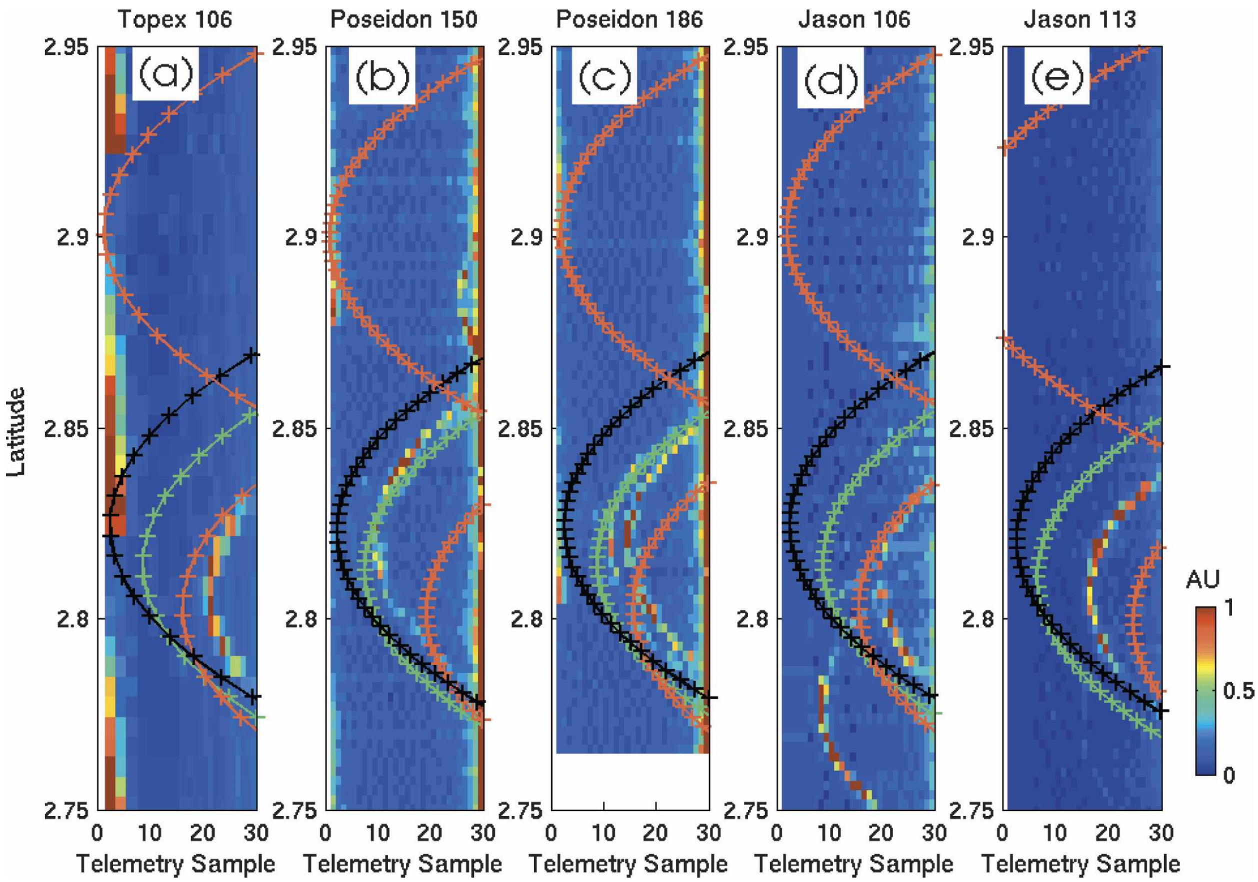

FIG. 4. Altimeter waveforms (normalized by the maximum value observed over the beacons) over the Straits of Malacca beacons for (a) TOPEX cycle 106, (b) Poseidon cycles 150 and (c) 186, and (d) Jason cycles 106 and (e) 113. The signatures of the beacons computed from the beacon and satellite coordinates are superimposed. The line colors correspond to the beacon colors of Fig. 3. The waveforms are normalized by the maximum value and the color scales are given in normalized units.

tude and range correspond to along-track and across-track positioning errors and can thus be used to estimate the accuracy of the satellite ground track positioning. For example, the shift is about two waveforms in latitude and about one telemetry sample in range for Poseidon cycle 150. Using (2), this corresponds to about a 500-m shift in latitude and a 120-m shift in range. A more precise computation could be done using the methods defined for transponders (Powell et al. 1993; Denys et al. 1995).

5. Small islands

Small island echoes are also often detected in high-rate waveforms. These islands or islets are, in general, not flagged for land in the sensor or geophysical data records (SDRs or GDRs) because they are either too small or located too far away from the satellite track. Figure 5 presents the echoes of the Paracels Islands in the South China Sea. The Paracels archipelago is composed of 130 small mainly low and flat coral islands and reefs. Pass 153 of TOPEX/Poseidon and Jason passes over the archipelago or more precisely over the western group of islands (Crescent group). These islets have marked signatures in altimeter waveforms that eventually lead to tracker loss near 16°33′N for cycles 7 and 8. The comparison of the islets signatures (computed from the coordinates of the satellite ground track and of the islands) represented as white parabolas to the waveforms shows no significant shift in latitude and range. One interesting feature is the "disappearance" of the northern group of islets in cycle 10 waveforms. The analysis of the GDR shows that the tide is about 0.2 m for cycle 10 compared to −0.4 m for cycle 8 and −0.2 m for cycle 7. The disappearance of the signature of the northern group, as well as the relative weakening of the southern group one, certainly results from the reduction of the uncovered surface at higher tide.

The last example is taken in Townsville Bay in Australia where two small islands, Rattlesnake and Herald,

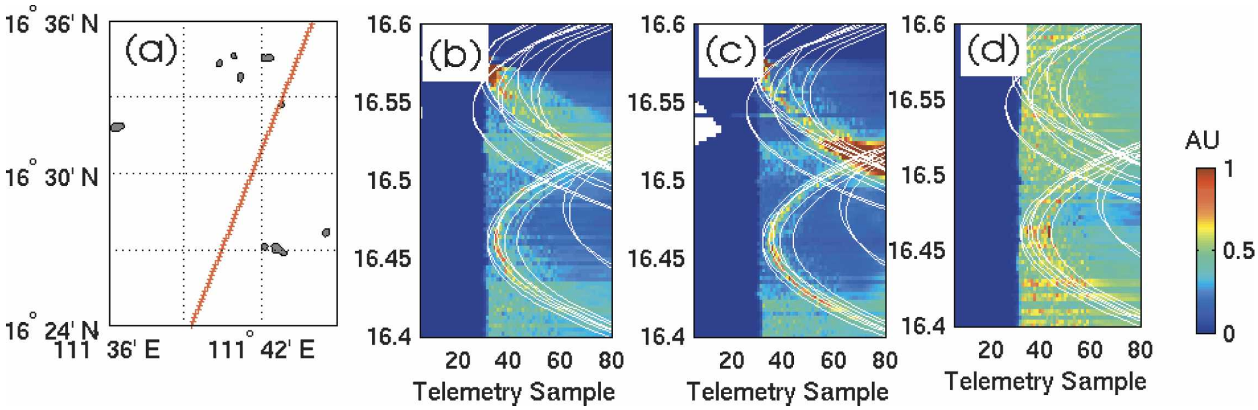

FIG. 5. Signature of Paracels Islands in Jason waveforms. (a) The Jason pass 153 ground track near the Paracels Islands. (b)–(d) Jason pass 153 for cycles 7, 8, and 10. The signatures estimated from satellite and island coordinates are superimposed as white lines. The waveforms are normalized by the maximum value and the color scales are given in normalized units.

(about 1 km long) are overflown by pass 175 of TOPEX and Jason. Only Herald Island, which lies close to the satellite track, has a discernible signature, as can be seen in Fig. 6. It is, in general, only discernable in the thermal section of the waveforms (e.g., cycles 7 and 8), but, sometimes, its signature becomes strong enough to affect the whole waveforms. For such cases, the waveforms take a land surface shape. This change of signature can also be attributed to tidal effects and to the associated uncovering of large surfaces. In this shallow water coastal zone, the tidal range is about 3 m and the GDR tides accuracy is not very good, so the tidal prediction for Townsville was used (from the Australian National Tide Facility). The tide was high for cycles 7 and 8 at 1.91 and 2.77 m, respectively, and low for cycle 10 at 1.37 m. At low tide the uncovered surface near Herald Island certainly increases and the proportion of land within the altimeter footprint becomes large enough to have a land surface return to the altimeter.

6. Perspectives: Potential applications

The signature of small targets, such as ships, beacons, and small islands, uncovered by the sea can have a discernible signature in high-resolution altimeter waveforms. This signature is purely deterministic and can be easily computed by simple geometric consideration in a similar way as the one used for transponders. It depends on the distance of the target from the satellite nadir and on the altitude of the target. The examples of signatures of ships, beacons, and islands of TOPEX/Poseidon and Jason presented show the precision of altimetric data as well as the wealth of information they contain. It is sometimes possible to distinguish a ship deck from the bridge, to detect beacons marking sea lanes, and to see the uncovering or covering of small islands by tides.

An obvious application of this study concerns an independent evaluation of the satellite ground track coordinates on a routine and cheap basis using selected beacons and small islands. The Straits of Malacca and Paracels Islands examples show the feasibility of such a control. A second application could be an evaluation of ship traffic on a global basis. As shown in the examples of section 3, ships give a detectable signature in the waveforms and this signature is confined in the thermal section of the waveforms. A detection algorithm based

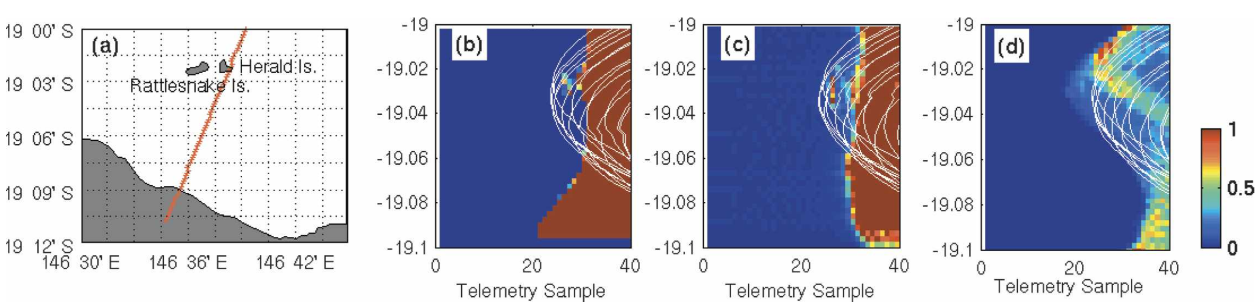

FIG. 6. Signature of small islets in Townville Bay, Australia. (a) The Jason pass 175 ground track near the islets. (b)–(d) Jason pass 175 for cycles 7, 8, and 10. The islets' signatures estimated from satellite and island coordinates are superimposed as white lines. The waveforms are normalized by the maximum value observed over the island and the color scales are given in normalized units.

on the analysis of the thermal section of the waveforms could be easily defined and the analysis of 1 yr of data could give an independent estimate of ship traffic around the globe (at least of its relative geographical distribution). In its 10-day repeat orbit, the Jason altimeter has the potential to detect up to 10% of large ships in the open ocean. A third application concerns coastal applications. Up to now the use of altimetry for coastal zone studies has been limited by problems of tracker and data losses during the land to sea transition and by the inaccuracy of tidal corrections. The analysis of the waveforms near the Paracels and in the Townsville Bay clearly shows that high-rate waveforms contain usable information on sea surface topography very close to the coast. They are also highly sensitive to tides and might be used as an independent validation tool for tide models in remote coastal zones.

Acknowledgments. The author wishes to thank the Centre National d'Etudes Spatiales (CNES) for financial support and the Centre AVISO for providing the altimeter's waveform data. Helpful comments from anonymous reviewers are also acknowledged.

REFERENCES

Barrick, D., and B. Lipa, 1985: Analysis and interpretation of altimeter sea echo. *Advances in Geophysics,* Vol. 27, Academic Press, 61–100.

Brown, G. S., 1977: The average impulse response of a rough surface and its applications. *IEEE Trans. Antennas Propag.,* **AP-25,** 67–74.

Denys, P. H., A. R. Birks, P. A. Cross, R. J. Powell, P. Pesec, and B. Burki, 1995: Transponder altimetry precise height measurements over land. *J. Geophys. Res.,* **100,** 24 347–24 359.

Legresy, B., F. Papa, F. Remy, G. Vinay, M. Van den Bosch, and O.-Z. Zanife, 2005: Envisat radar altimeter measurements over continental surfaces and ice caps using the ICE-2 retracking algorithm. *Remote Sens. Environ.,* **95,** 150–163.

Powell, R. J., A. R. Birks, W. J. Wrench, and C. L. Biddiscombe, 1993: Using transponders with ERS-1 and TOPEX altimeters to measure orbit altitude to ±3 cm. *Proc. First ERS-1 Symp. (ESA SP-359),* Cannes, France, ESA, 511–516.

Quartly, G. D., 1998: Determination of oceanic rain rate and rain cell structure from altimeter waveform data. Part I: Theory. *J. Atmos. Oceanic Technol.,* **15,** 1361–1378.

——, M. A. Srokosz, and A. C. McMillan, 2001: Analyzing altimeter artifacts: Statistical properties of ocean waveforms. *J. Atmos. Oceanic Technol.,* **18,** 2074–2091.

Roca, M., H. Jackson, and C. Celani, 2003: RA-2 sigma-0 absolute calibration. *Proc. Envisat Validation Workshop (ESA SP-531),* Frascati, Italy, ESA, CD-ROM.

Tournadre, J., 1998: Determination of rain cell characteristics from the analysis of TOPEX. *J. Atmos. Oceanic Technol.,* **15,** 387–406.

——, B. Chapron, N. Reul, and D. C. Vandemark, 2006: A satellite altimeter model for ocean slick detection. *J. Geophys. Res.,* **111,** C04004, doi:10.1029/2005JC003109.